Journal of the European Ceramic Society **13** (1994) 313–321

Influence of Oxidation in SO_2–Air Mixtures on the Room-Temperature Strength of Silicon Nitride

Jean-Bernard Veyret, Richard J. Fordham

Institute for Advanced Materials, Commission of the European Communities, Petten, The Netherlands

&

Michel Billy

Laboratoire de Céramiques Nouvelles, University of Limoges, Limoges, France

(Received 5 July 1993; accepted 15 October 1993)

Abstract

The influence of oxidation in SO_2–air mixtures on the mechanical properties of two hot-pressed and one pressureless sintered Si_3N_4 ceramics was investigated. Samples were corroded for 25 h in the range 800–1500°C in 1 vol.% SO_2 in dry air and the residual flexural strength was measured at room temperature. In SO_2, the dominant reaction process is oxidation, accompanied by reaction of sulphur oxides with the surface oxide layers, to yield sulphates where these are stable under the experimental conditions. This sulphate formation appears not to affect the mechanical strength of silicon nitride.

Der Oxydationseinfluß eines SO_2–Luft-Gemischs auf die mechanischen Eigenschaften zweier heißgepreßter Si_3N_4-Keramiken und einer drucklos gesinterten Si_3N_4-Keramik wurde untersucht. Die Proben wurden 25 Stunden lang in einem Temperaturbereich von 800–1500°C in trockener Luft mit einem 1 Vol.% Anteil SO_2 korrodiert und die Eigendurchbiegefestigkeit bei Raumtemperatur gemessen. Der dominierende Prozeß in SO_2–Luft ist die Oxidation, begleitet von einer Reaktion des Schwefeloxids mit der Oberflächenoxidschicht zu Sulphaten, bei Bedingungen, bei denen diese stabil sind. Die Sulphatbildung beeinflußt offenbar nicht die mechanische Festigkeit des Silziumnitrids.

Nous avons étudié l'influence de l'oxydation en atmosphère de SO_2 mélangé à de l'air sur les propriétés mécaniques de céramiques de Si_3N_4, dont deux étaient pressées à chaud et une frittée naturellement. Les échantillons ont été oxydés 25 heures entre 800 et 1500°C dans un mélange d'air sec et de 1% vol. de SO_2, puis la résistance à la flexion a été mesurée à température ambiante. Dans le mélange SO_2–air, la réaction la plus importante est l'oxydation accompagnée d'une réaction des oxydes de soufre avec les couches d'oxyde en surface, ce qui conduit à la formation de sulfates stables pour ces conditions expérimentales. Le sulfate formé ne semble pas affecter la résistance mécanique du nitrure de silicum.

1 Introduction

In view of its high strength and oxidation resistance up to 1500°C, silicon nitride is one of the most important candidates for high-temperature applications for structural components in a number of advanced applications such as gas turbine or diesel engines.

The oxidation behaviour of sintered or hot-pressed materials is expected to differ according to the sintering additives used (MgO, Al_2O_3, Y_2O_3).[1] Much work has been devoted to characterizing the behaviour of silicon nitride in pure oxidizing atmospheres. It is now well recognized that the use of yttria as a densification aid for Si_3N_4 sintering results in the formation of highly refractory secondary phases, improving the high-temperature strength behaviour[2–8] compared with Si_3N_4 densified with MgO.[9–15]

The properties of silicon nitride in complex environments have received little attention. The effect of the combustion of fuels becomes more aggressive as the level of contaminants increases

Journal of the European Ceramic Society 0955-2219/94/$7.00

with decreasing fuel quality[16] and in a number of industrial operations ceramics must operate under conditions in which the gas phase contains sulphur.

The objectives of the present work were to characterize the influence of additives on the room temperature strength behaviour of three silicon nitrides after corrosion in 1 vol.% SO_2–air for 25 h at different temperatures in the range 800–1500°C.

2 Experimental Procedure

Two commercial materials, coded SN1 (Ceranox NH209) and SN2 (Ceranox NH206) and one non-commercial material coded SN3 were supplied by Feldmühle AG, Germany. SN1 and SN2 were hot-pressed at 1750°C under 40 MPa pressure with 9 wt% yttria and 1·2 wt% magnesia respectively. SN3 was sintered under normal nitrogen pressure at 1650°C with a mixture of 10 wt% yttria and 1·2 wt% magnesia. Table 1 gives the material composition supplied by the manufacturer and the main microstructural characteristics of the materials.

Corrosion exposures were performed in a specially designed horizontal furnace between 800 and 1500°C in 1 vol.% SO_2/air (P=1 atm) for 25 h. Table 2 gives calculated partial pressures of O_2, SO_2 and SO_3 as a function of temperature, assuming thermodynamic equilibrium (thermodynamic calculations were made using data from Barin & Knacke[17]). A Pt catalyst in the hot zone of the furnace upstream of the specimens was used to ensure equilibrium conditions.

Room-temperature flexural strengths (σ_F) were measured by four-point bending, with a support span of 40 mm, a loading span of 20 mm and a crosshead speed of 0·5 mm min^{-1} on 3·5 × 4·5 × 50 mm^3 bars machined, ground and finally polished on the tensile face; the edges were chamfered (lengthwise) to prevent notch effects. The phases present on the surface were identified by X-ray diffraction and the morphology of fracture surfaces was examined by SEM.

Table 1. Materials

	HPSN (SN1)	*HPSN (SN2)*	*SSN (SN3)*
Composition (mass %—balance Si_3N_4)			
Y_2O_3	9·0	0·005	10·0
MgO	0·01	1·2	1·2
Fe_2O_3	1·7	2·7	0·1
ZrO_2	0·01	0·01	1·6
Al_2O_3	0·12	0·2	0·2
CaO	0·05	0·25	0·06
Open porosity (%)	0·2	0	4·10
Apparent density (g cm^{-3})	3·33	3·2	3·15
Main phases identified by X-ray diffraction	β-Si_3N_4 $Y_{10}Si_7O_{23}N_4$ $FeSi_2$	β-Si_3N_4 Mg_2SiO_4 FeSi	β-Si_3N_4 α-Si_3N_4 $Y_{10}Si_7O_{23}N_4$
TEM analysis at grain boundaries	$Y_{10}Si_7O_{23}N_4$	Glassy phase Mg_2SiO_4 FeSi	Glassy phase $Y_{10}Si_7O_{23}N_4$

Table 2. Partial pressure of O_2, SO_2 and SO_3 as function of temperature in 1 vol.% SO_2–air mixture (atm)

Temperature (°C)	p_{O_2}	p_{SO_3}	p_{SO_2}	p_{SO_2}/p_{SO_3}
800	0·26	$3·0 \times 10^{-3}$	$6·9 \times 10^{-3}$	2·30
900	0·26	$1·4 \times 10^{-3}$	$8·5 \times 10^{-3}$	6·07
1000	0·26	$7·3 \times 10^{-4}$	$9·2 \times 10^{-3}$	12·60
1175	0·26	$2·2 \times 10^{-4}$	$9·7 \times 10^{-3}$	44·09
1300	0·26	$1·3 \times 10^{-4}$	$9·8 \times 10^{-3}$	75·38
1400	0·26	$9·1 \times 10^{-5}$	$9·9 \times 10^{-3}$	108·7

3 Results

3.1 Non-corroded samples

20 bars of SN1 and 10 bars each of SN2 and SN3 were tested in four-point bending at room temperature to measure the reference strength. A statistical variation of fracture strength, σ_F, against probability of survival (so-called Weibull plot) is shown in Fig 1. SN1 and SN2 have identical average strengths of 610 MPa, whereas SN3 showed a lower value of 470 MPa. The relatively high values, for ceramics, of the Weibull modulus (m) for SN1 and SN2, 20 and 15, respectively, illustrate a low level of critical defects and good microstructural homogeneity.

Examination of the fracture surface of SN3 by SEM with EDAX analysis revealed failure initiating sites such as iron-rich inclusion flaws originating from processing (Fig. 1). The important open porosity of SN3 (4·1%) is also a likely reason for the lower Weibull modulus of SN3 (m = 10).

3.2 Corroded samples

The oxidation products identified by XRD after 25 h exposure are reported in Table 3.

The examination by SEM with EDAX analysis of the oxidized surfaces of SN1, SN2 and SN3 (Fig. 2) showed the presence of sulphur associated with cations originating from additives and impurities. As no sulphates were identified by X-ray analysis, ESCA was performed on all samples and the presence of sulphur as S^{6+} (sulphate) was indicated. This was confirmed by washing the samples with distilled water, after which sulphur was no longer detectable on the surface. The soluble products identified by XRD are reported in Fig. 3 which shows the quantity of sulphate dissolved by water as a function of temperature. The maximum sulphate formation was found at 800°C for SN1

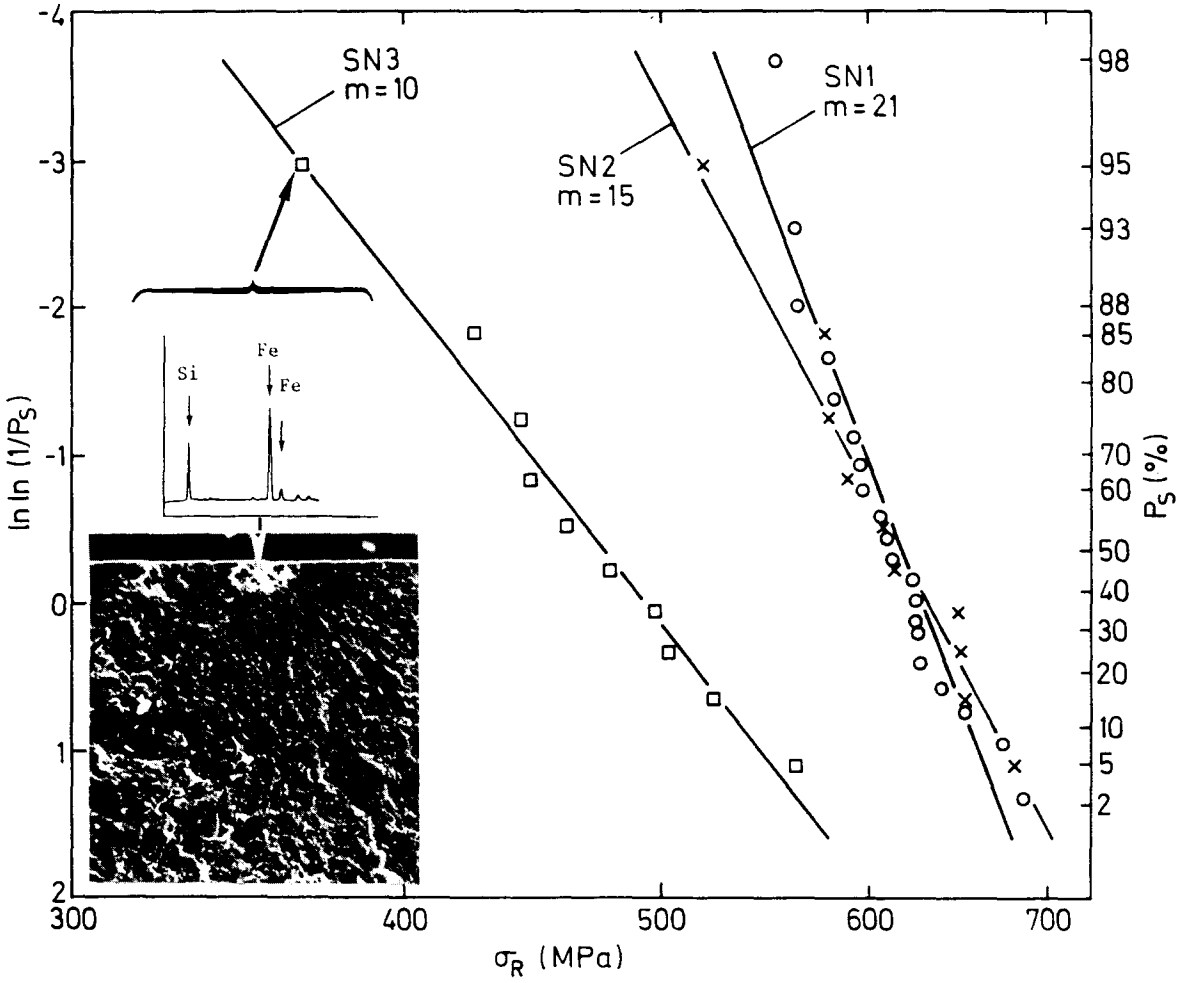

Fig. 1. Weibull distributions for unexposed materials.

and 1200°C for SN2 and SN3. Above 1300°C no sulphates were found.

3.3 Residual strength measurements

Residual flexural strength and percentage weight change were measured at room temperature on 10 bars after exposure in SO_2–air (1 vol. %) for 25 h between 800 and 1500°C for SN1 (Fig. 4), SN2 (Fig. 6) and SN3 (Fig. 8).

For SN1, σ_F decreases gradually from 900°C to a minimum at 1300°C. A sudden increase in σ_F was recorded from 1300°C up to 1500°C, where the average strength value of 630 MPa is similar to the value of 610 MPa for exposed material. Examination of fracture surfaces by SEM for 800°C and 1200°C exposures are shown in Fig. 5.

Sulphur appears strongly in the low-temperature range (800–900°C) as is illustrated in Fig. 5(a). Small humps rich in sulfur and yttrium were observed on the surface of the samples. These humps correspond to yttrium sulphate $Y_2(SO_4)_3$ detected by XRD analysis. After exposure at 1200°C, the morphology of the surface remains identical. The observation of a duplex oxide–sulphate scale (Fig. 5(b)) shows the sulphur did not penetrate the oxide scale.

For SN2 (Fig. 6), a sudden decrease in strength to 515 MPa was observed for the samples corroded at 1000°C relative to unexposed material (615 MPa). This value remained constant up to 1200°C, above which temperature a continuous decrease in σ_F was observed up to 1500°C. An examination of the fracture surface of a sample oxidized at 1300°C is shown in Fig. 7. The initial fracture site is a pit and sulphur is seen to be identified associated with calcium.

For SN3, at low temperature (900°C), the rupture strength is proved (527 MPa), compared to non-corroded samples (470 MPa) (Fig. 8). Between 1100 and 1300°C, the rupture strength is

Table 3. Oxidation products (oxides and silicates) identified by XRD on SN1, SN2 and SN3 after 25 h exposure in 1 vol.% SO_2–air at different temperatures

	800°C	*1000°C*	*1100–1200°C*	*1300–1500°C*
SN1	$Y_{4.67}(SiO_4)_3O$ SiO_2[a] $Y_2Si_2O_7$		$Y_2Si_2O_7$ SiO_2[a]	
SN2	SiO_2[a] $CaMg(SiO_3)_2$	SiO_2[a] $CaMg(SiO_3)_2$ $MgSiO_3$	SiO_2[a] $MgSiO_3$ $CaFeMgSi_2O_6$	
SN3	SiO_2[a] $Y_2Si_2O_7$	SiO_2[a] $Y_2Si_2O_7$ $MgSiO_3$	SiO_2[a] $Y_2Si_2O_7$ $MgSiO_3$ $Ca_2Al_2SiO_7$	

[a] Cristobalite.

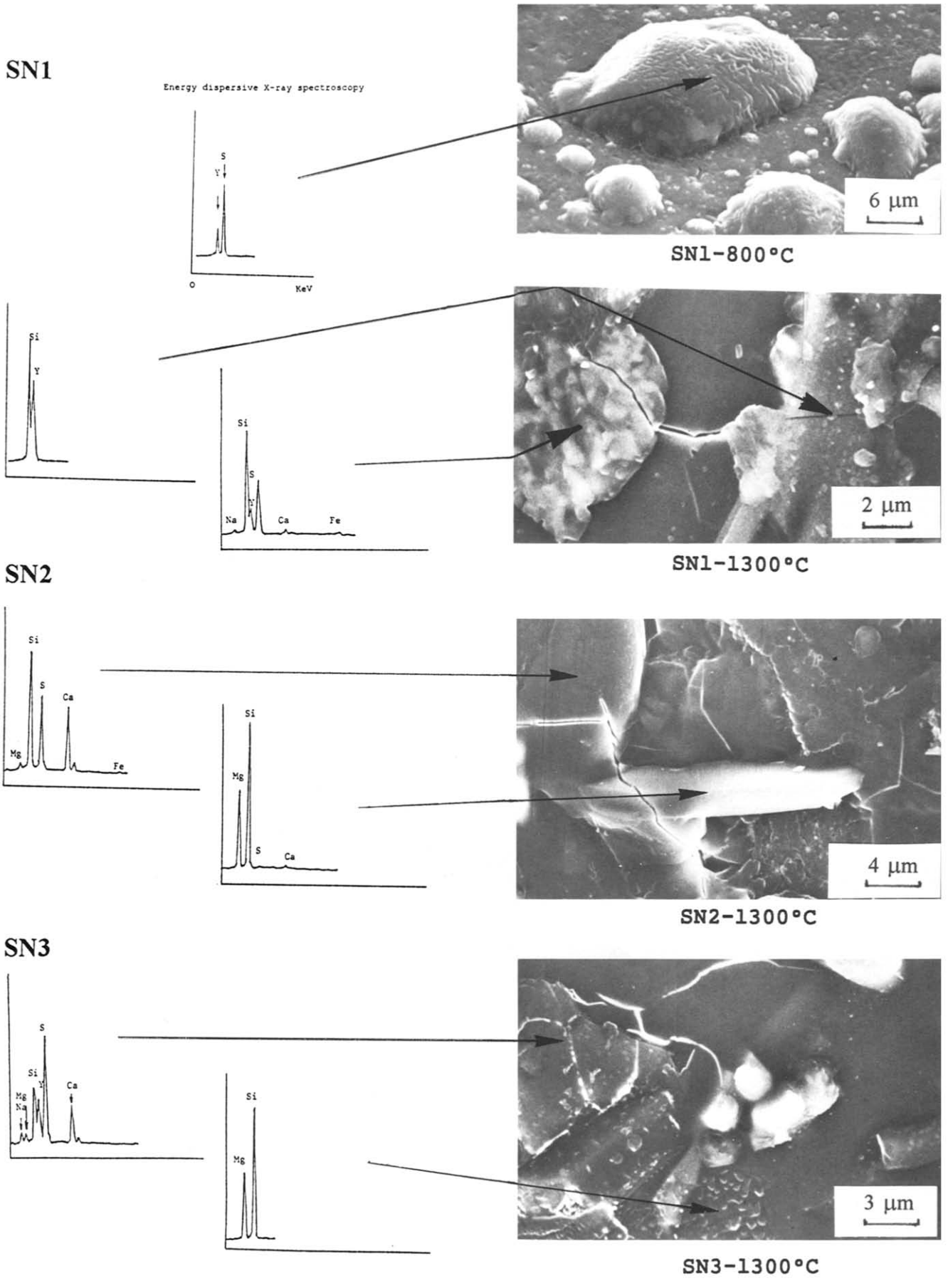

Fig. 2. SEM of the surface of 25 h corroded SN1, SN2 and SN3 samples in 1 vol.% SO_2–air at different temperatures.

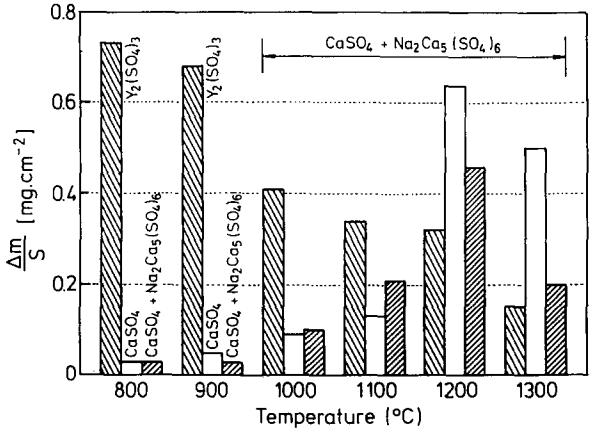

Fig. 3. Weight loss and identified productions after washing (▨) SN1, (▨) SN2 and (□) SN3 samples exposed for 10 h in 1 vol.% SO_2–air at different temperatures.

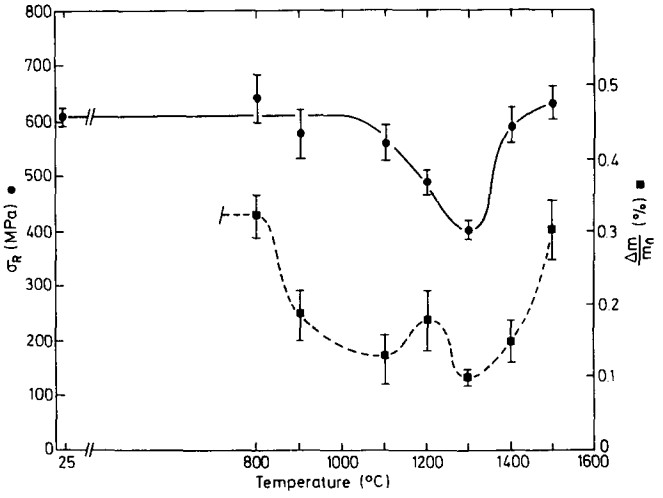

Fig. 4. Room temperature flexural strength of 25 h corroded SN1 samples in 1 vol.% SO_2–air at different temperatures.

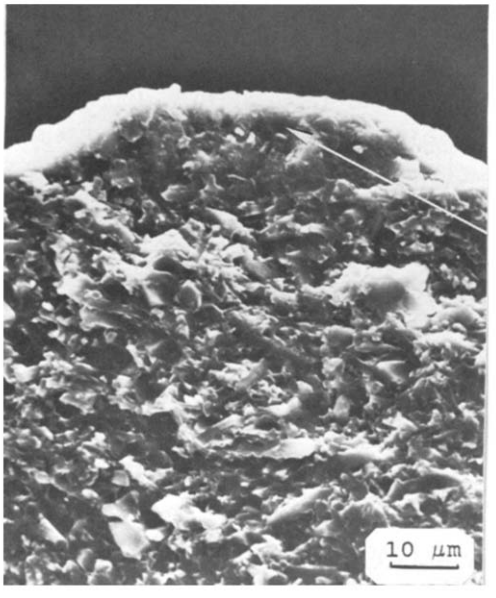

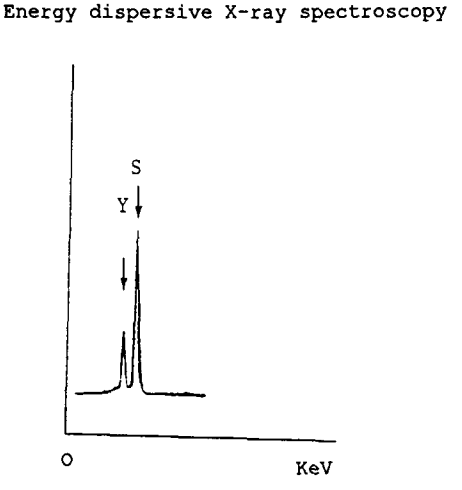

(a)

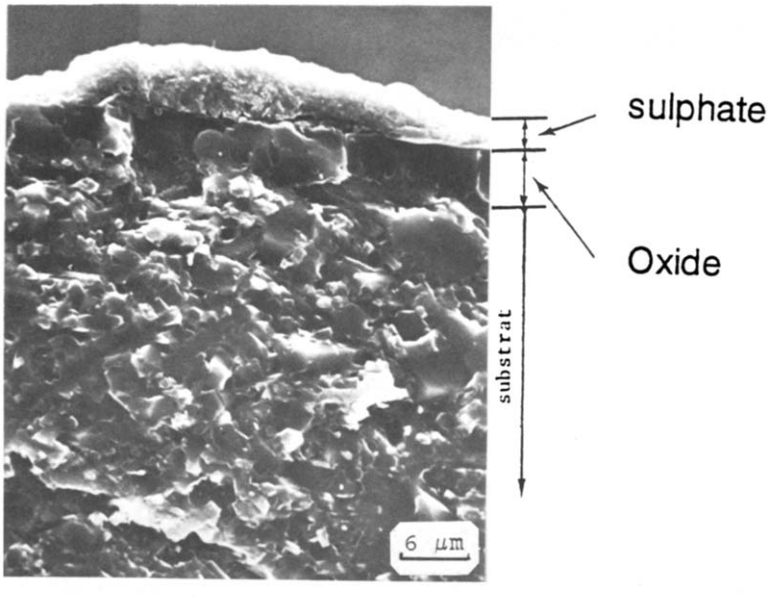

(b)

Fig. 5. Fracture surfaces for SN1 specimens exposed to 1 vol.% SO_2–air for 25 h at (a) 800°C and (b) 1200°C.

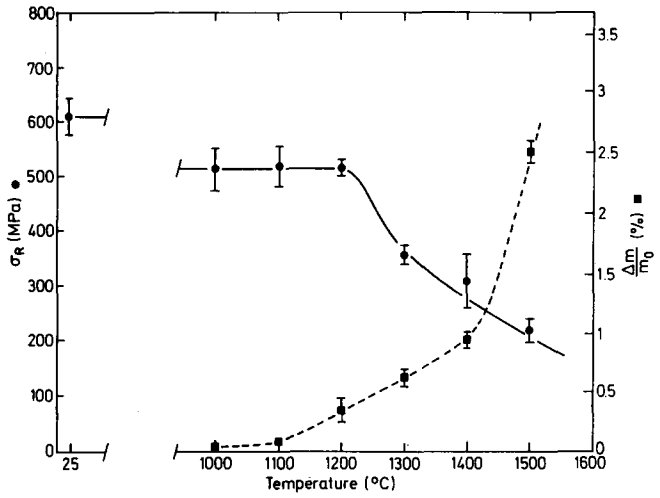

Fig. 6. Room temperature flexural strength of 25 h corroded SN2 samples in 1 vol.% SO_2–air at different temperatures.

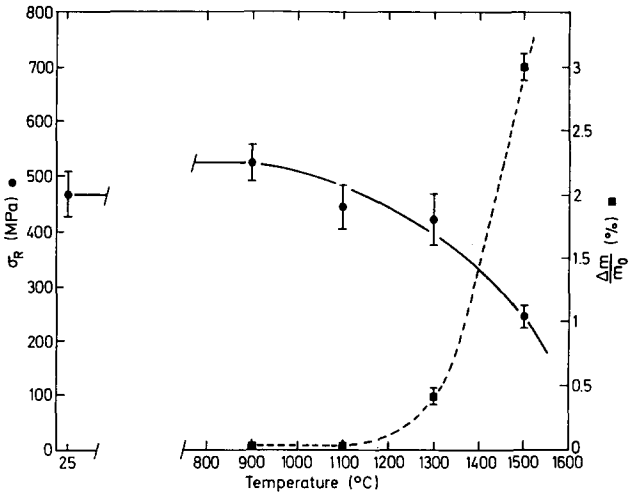

Fig. 8. Room temperature flexural strength of 25 h corroded SN3 samples in 1 vol.% SO_2–air at different temperatures.

similar to the room-temperature value but decreases significantly above 1300°C. SEM examination of the rupture surface of samples from 1300°C did not reveal any sulphate formation. The presence of macro-pores (Fig. 9(a)) and an irregular oxide–nitride interface associated with high porosity (Fig. 9(b)) were noted.

4 Discussion

Under these experimental conditions, SiO_2 is the expected stable species over Si_3N_4. However, we can expect a reaction between sulphur oxides and the cations concentrated at grain boundaries.

Figure 10 (redrawn from Ref. 18) shows super-

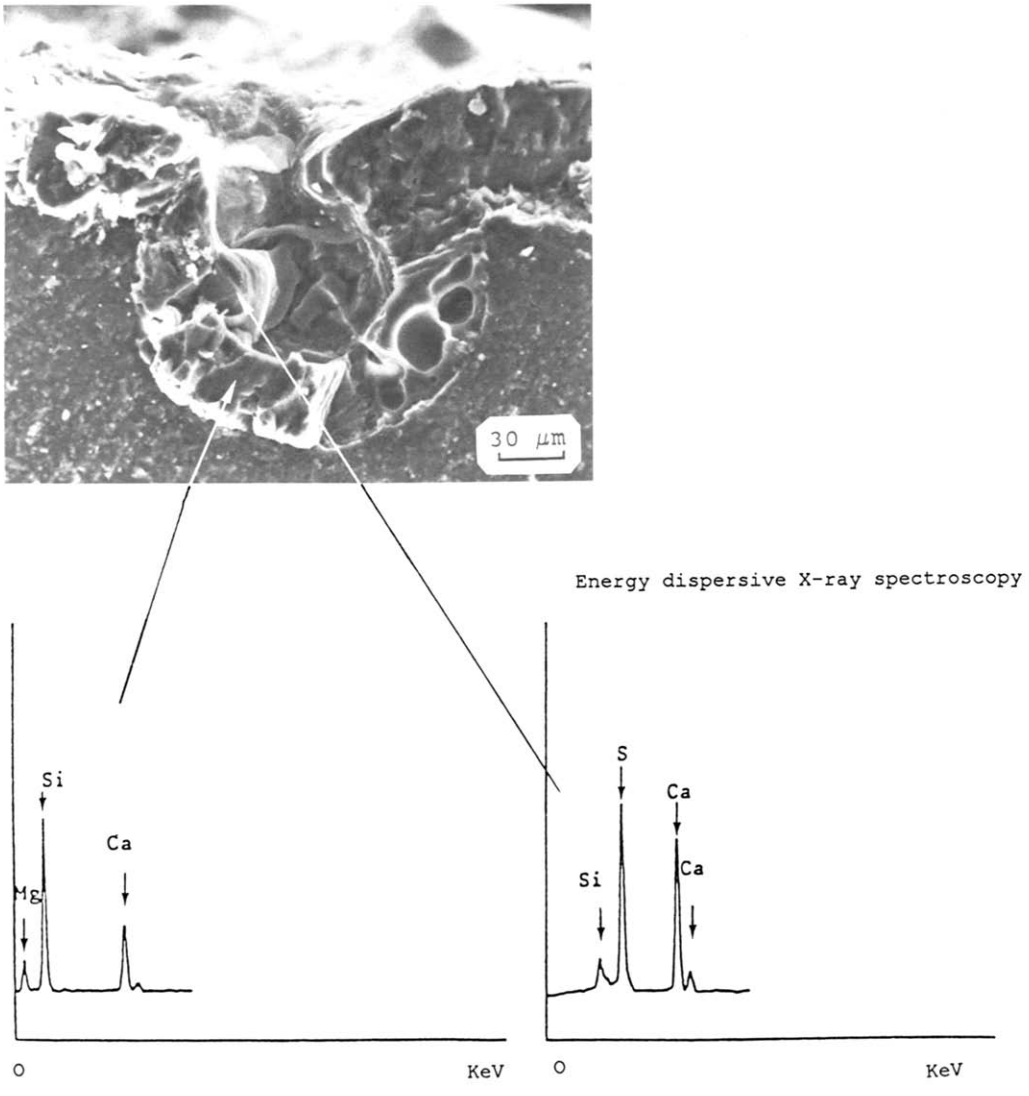

Fig. 7. Fracture surface for SN2 specimen exposed in 1 vol.% SO_2–air for 25 h at 1300°C.

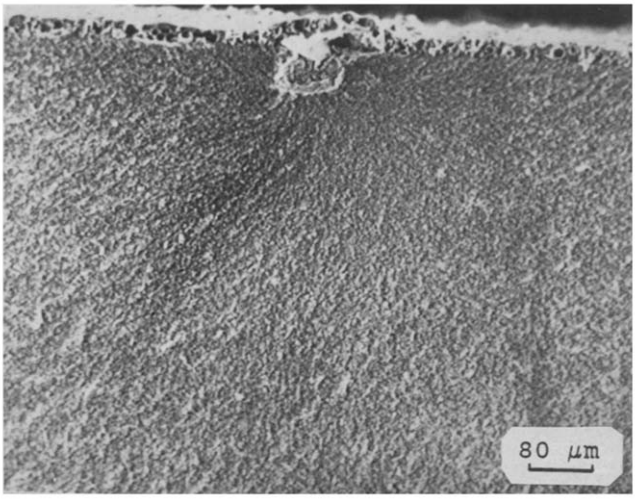

(a)

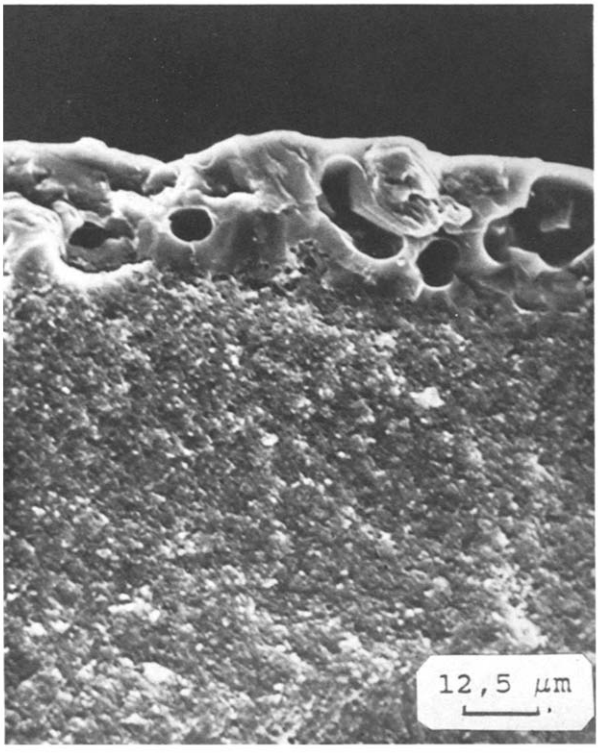

(b)

Fig. 9. Fracture surface for SN3 specimen exposed in 1 vol.% SO_2–air for 25 h at 1300°C.

imposed stability diagrams calculated for M–O–S systems (with M = Fe, Al, Mg, Ca and Na) at 1450 K (1177°C).

From these diagrams, it is clear that in 1 vol.% SO_2–air at this temperature, the SO_3 partial pressure is high enough to permit the formation of Na_2SO_4 and $CaSO_4$ but not $Fe_2(SO_4)_3$, $Al_2(SO_4)_3$ and $MgSO_4$. Raising the temperature has the effect of moving the boundary between M_xO_y and $M_x(SO_4)_y$ upwards. Lowering the temperature reverses this effect. The result at higher temperature will be to prevent the formation of $CaSO_4$ and eventually Na_2SO_4. In the absence of thermodynamic data for Y–O–S, pure Y_2O_3 was exposed in 1 vol.% SO_2–air under slowly increasing temperature; $Y_2(SO_4)_3$ was formed and decomposed at 1000°C. Although the calculations are based on pure oxides, the formation of mixed sulphates can be anticipated. The temperature stability of some sulphates is given in Table 4.

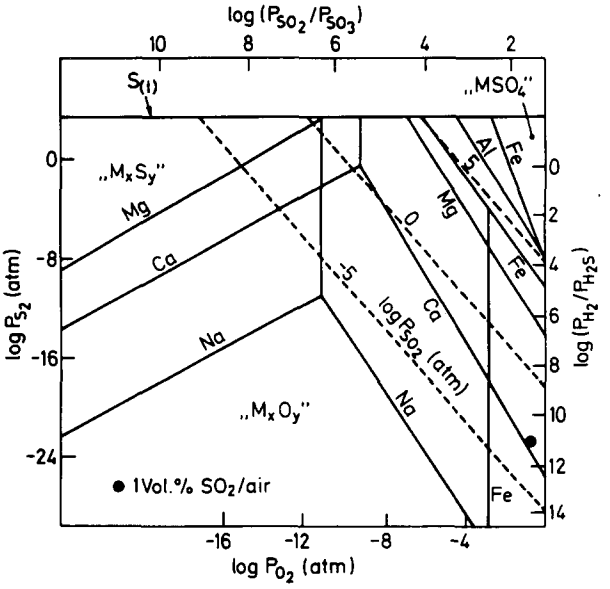

Fig. 10. Stability diagram for M–O–S systems with M = Fe, Al, Mg, Ca and Na (from Ref. 18).

Previous kinetic studies[19,20] have shown that in SO_2–air the dominant reaction process is oxidation with the formation of an oxide scale identical to the one formed in air, but accompanied by reactions of sulphur oxides at the surface oxide layers to yield sulphates, where these are stable under the experimental conditions. Sulphur did not penetrate the bulk material and not even the oxide scale.

The mechanical behaviour of SN1 confirms the kinetic studies performed in air[19] and in SO_2–air.[20] The intergranular oxidation of the H-phase ($Y_{10}Si_7O_{23}N_4$),[21] confirmed by the relatively high value of weight gain at 800°C and by the presence of yttrium silicates on the oxidised surface, is responsible for the slow decrease in σ_F at 900°C; intergranular attack induces superficial microcracks which are probably the origin of failure. This effect is seen up to 1300°C. Above 1300°C, the silicon nitride grains oxidize to form a protective oxide scale which can act as an oxygen diffu-

Table 4. Properties of some sulphates

	Melting point (°C)	*Decomposition temperature* (°C) *at 1 atm in air*
Na_2SO_4	884	—
$CaSO_4$	1 450	—
$CaMg_3(SO_4)_2$	1 210	—
$MgSO_4$	—	1 124
$Y_2(SO_4)_3$	—	1 000
$Al_2(SO_4)_3$	—	770

sion barrier. The oxidation of the H-phase is blocked by a silica film which seals off the surface defects. The improvement of mechanical properties at high temperature (>1300°C) is due both to the refractory nature of the grain boundary phase (H-phase) and to the protective nature of the oxide film (compatibility between $Y_2Si_2O_7$ and SiO_2).

Finally the reactivity of sulphur is a surface effect; sulphur does not penetrate the bulk material and not even the oxide scale. The mechanisms of rupture for SN1 are not induced by the sulphate formation but only by the oxidation process.

The oxidation behaviour of SN2 in air and in SO_2–air (1 vol.%) has also been previously reported.[19,20] The outward diffusion of cations and impurities, especially liquid silicate-forming elements, appeared to be the most likely rate-limiting step with inward oxygen diffusion taking place through pores and cracks of the multicomponent oxide scale.

In SO_2–air, the grain boundary diffusion mechanism is coupled with an external reaction with SO_x. The reaction with sulphur results from an interaction with a glassy phase containing calcium. For this reason the phenomenon is significant only at temperatures where the glassy phase becomes mobile and susceptible to devitrification in contact with SO_x at the outer surface. Sulphate formation was a secondary phenomenon which did not modify the oxidation mechanism.

The decrease in strength up to 1200°C may be linked to an internal oxidation of the grain boundary phases in relation to ionic mobility.[1] Above 1200°C, the oxidation starts to be significant and a new fracture mechanism predominates, which may be attributed to new strength-controlling defects like pits. In this temperature range the oxidation of the nitride also becomes important, the oxide is cracked and the oxide–substrate interface is irregular.

The SN3 material contains an Y–N apatite ($Y_{10}Si_7O_{23}N_4$) and a nitrogen glassy phase rich in yttrium and magnesium. At low temperature (800–1000°C), this glassy phase appeared to protect the Y–N apatite against oxidation,[20] which may explain the absence of the Y–N apatite phase oxidation observed with SN1. At low temperature (900°C), the formation of a thin silica film seals off the spherical defects, improving the rupture strength. Between 1100 and 1300°C, the high melting temperature of the vitreous phase (because of yttrium) decreases the mobility of cations. It is only above 1300°C that the rupture strength decreases because diffusion of additives and impurities are predominant. There is a dissolution of the nitride at the internal interface by the silicate, and the oxide–nitride interface becomes irregular.

The rupture of SN3 is finally governed by pre-existing defects and by an irregular oxide–nitride interface, whilst the release of nitrogen and the internal interface creates a high porosity oxide scale.

5 Conclusions

Complex environments such as SO_2–air do not affect the overall rate control of oxidation. The reaction of sulphur oxides occurs at the surface of oxide layers to yield sulphates, where these are stable under the experimental conditions. The influence of sulphur in oxidizing atmospheres is not to be feared; and the mechanical properties are only affected by oxidation.

Acknowledgements

The authors thank P. Glaude, K. Schuster and P. Frampton for the microstructural investigations.

References

1. Billy, M. & Desmaison, J. G., High-temperature oxidation of silicon-based structural ceramics. *High-Temp. Tech.*, **4** (1986) 131–9.
2. Lange, F. F., Phase relations in the system Si_3N_4–SiO_2–MgO and their interrelation with strength and oxidation. *J. Am. Ceram. Soc.*, **61** (1978) 53–6.
3. Lange, F. F., Eutectic studies in the system Si_3N_4–Si_2N_2O–Mg_2SiO_4. *J. Am. Ceram. Soc.*, **62** (1979) 617–19.
4. Kossowsky, R., The microstructure of hot pressed silicon nitride. *J. Mater. Sci.*, **8** (1973) 1603–15.
5. Iskoe, J. L., Lange, F. F. & Diaz, E. S., Effect of selected impurities on the high temperature mechanical properties of hot-pressed silicon nitride. *J. Mater. Sci.*, **11** (1976) 908–12.
6. Lange, F. F., Singhal, S. C. & Kuznicki, R. C., Phase relations and stability studies in the Si_3N_4–SiO_2–Y_2O_3 pseudoternary system. *J. Am. Ceram. Soc.*, **60** (1977) 249–52.
7. Sanders, W. A & Mieskowski, D. M., Strength and microstructure of sintered Si_3N_4 with rare-earth-oxide additions. *Am. Ceram. Soc. Bull.*, **64** (1985) 304–9.
8. Gauckler, L. J., Hohnke, H. & Tien, T. Y., The system Si_3N_4–SiO_2–Y_2O_3. *J Am. Ceram. Soc.*, **63** (1980) 35–7.
9. Tsuge, A., Nishida, K. & Komatsu, M., Effect of crystallizing the grain boundary glass phase containing Y_2O_3. *J. Am. Ceram. Soc.*, **58** (1975) 323–6.
10. Smith, J. T. & Quackenbush, C. L., Phase effects in Si_3N_4 containing Y_2O_3 or CeO_2: I, strength. *A. Ceram. Soc. Bull.*, **59** (1980) 529–32.
11. Babini, G. N., Bellosi, A. & Vincenzini, P., A diffusion model for the oxidation of hot pressed Si_3N_4–SiO_2–Y_2O_3 materials. *J. Mater. Sci.*, **19** (1984) 1029–42.
12. Mieskowski, D. M. & Sanders, W. A., Oxidation of silicon nitride sintered with rare earth oxide additions. *J. Am. Ceram. Soc.*, **68** (1985) C-160–C-163.
13. Singhal, S. C., Oxidation of silicon nitride and related

materials. In *Progress in Nitrogen Ceramics NATO(ASI), Series E: Applied Science*, No. 23F, ed. F. L. Riley. Martins Nijhoff, The Hague, The Netherlands, 1977, pp. 670–26.
14. Govila, R. K., Strength characterization of yttria-doped sintered silicon nitride. *J. Mater. Sci.*, **20** (1985) 4345–53.
15. Goursat, P., Dumazeau, E. & Billy, M., Oxidation of hot-pressed silicon oxynitride–yttria ceramics. In *Environmental Degradation of High Temperature Materials*, Series 3, Vol. 2. The Institution of Metallurgists. Northway House, Whetstone, London, 1979, pp. 15–20.
16. Morbioli, R. & Walter, P., Corrosion of superalloys: turbine blades. In *High Temperature Corrosion of Materials*, ed. G. Beranger, J. C. Colson & F. Dabois. CNRS, Paris, 1987, pp. 725–37.
17. Barin, I. & Knacke, O., *Thermochemical Properties of Inorganic Substances*. Springer-Verlag, Berlin, 1973.
18. Gulbrasen, E. A. & Meier, G. H., Rpt No. DOE/FE/13547-01, 1980.
19. Veyret, J. B. & Billy, M., Oxidation of hot-pressed silicon nitride: modelling. In *Euro-Ceramics*, Vol. 3, *Engineering Ceramics*, ed. G. de With, R. A. Terpstra & R. Metselaar. Elsevier Applied Science, Maastricht, The Netherlands, 1989, pp. 512–16.
20. Veyret, J. B., Fordham, R. J. & Billy, M., Oxidation behaviour of liquid phase sintered silicon nitride in SO_2/air mixtures (in press).
21. Veyret, J. B., Van De Voorde, M. & Billy, M., Oxidation behaviour of silicon yttrium oxynitride. *J. Am. Ceram. Soc.*, **75** (1992) 3289–92.